

Neurexin-1 β Binding to Neuroligin-1 Triggers the Preferential Recruitment of PSD-95 versus Gephyrin through Tyrosine Phosphorylation of Neuroligin-1

Grégory Giannone,^{1,2,3} Magali Mondin,^{1,2,3} Dolores Grillo-Bosch,^{1,2} Béatrice Tessier,^{1,2} Edouard Saint-Michel,^{1,2} Katalin Czöndör,^{1,2} Matthieu Sainlos,^{1,2} Daniel Choquet,^{1,2,4,*} and Olivier Thoumine^{1,2,4,*}

¹University Bordeaux

²CNRS

Interdisciplinary Institute for Neuroscience, UMR 5297, F-33000 Bordeaux, France

³These authors contributed equally to this work and are co-first authors

⁴These authors contributed equally to this work and are co-last authors

*Correspondence: dchoquet@u-bordeaux2.fr (D.C.), othoumin@u-bordeaux2.fr (O.T.)

<http://dx.doi.org/10.1016/j.celrep.2013.05.013>

SUMMARY

Adhesion between neurexin-1 β (Nrx1 β) and neuroligin-1 (Nlg1) induces early recruitment of the postsynaptic density protein 95 (PSD-95) scaffold; however, the associated signaling mechanisms are unknown. To dissociate the effects of ligand binding and receptor multimerization, we compared conditions in which Nlg1 in neurons was bound to Nrx1 β or non-activating HA antibodies. Time-lapse imaging, fluorescence recovery after photobleaching, and single-particle tracking demonstrated that in addition to aggregating Nlg1, Nrx1 β binding stimulates the interaction between Nlg1 and PSD-95. Phosphotyrosine immunoblots and pull-down of gephyrin by Nlg1 peptides *in vitro* showed that Nlg1 can be phosphorylated at a unique tyrosine (Y782), preventing gephyrin binding. Expression of Nlg1 point mutants in neurons indicated that Y782 phosphorylation controls the preferential binding of Nlg1 to PSD-95 versus gephyrin, and accordingly the formation of inhibitory and excitatory synapses. We propose that ligand-induced changes in the Nlg1 phosphotyrosine level control the balance between excitatory and inhibitory scaffold assembly during synapse formation and stabilization.

INTRODUCTION

Understanding the mechanisms that lead to the differential assembly of excitatory and inhibitory synapses is a fundamental goal in neurobiology. Synaptogenesis is a complex, multistep process that occurs at axon-dendrite contacts and is initiated by adhesion proteins followed by the recruitment of scaffolding proteins and functional receptors (Friedman et al., 2000). The molecules postsynaptic density protein 95 (PSD-95) and gephyrin are among the earliest hallmarks of excitatory and inhibi-

tory postsynaptic differentiation, respectively (Bresler et al., 2001; Washbourne et al., 2002; Gerrow et al., 2006; Pouloupoulos et al., 2009), and thus it is essential to identify the mechanisms that control their specific recruitment at novel neuronal contacts.

Among regulatory molecules, the postsynaptic adhesion molecules neuroligins (Nlgs) bind presynaptic neurexins (Nrxs) through their extracellular domain (Südhof, 2008). Nlgs interact intracellularly with PSD-95 through their C-terminal PDZ domain-binding motif (Irie et al., 1997) and with gephyrin through a consensus sequence located in the middle of the Nlg intracellular domain (Pouloupoulos et al., 2009). Studies in culture systems have shown that Nrxs and Nlgs are critical players in synapse initiation and maturation (Craig and Kang, 2007). Overexpressing Nlg1 in neurons promotes synapse formation, whereas silencing Nlgs reduces synapse number (Chih et al., 2005; Levinson et al., 2005; Ko et al., 2009; Chen et al., 2010). Furthermore, cocultured heterologous cells expressing Nlg1 or Nrx1 β induce pre- and postsynapses, respectively, in contacting neurites (Scheiffele et al., 2000; Graf et al., 2004; Nam and Chen, 2005). Nlgs can assemble both excitatory and inhibitory synapses, with the balance between them being regulated by the respective expression levels of PSD-95 and gephyrin (Graf et al., 2004; Chih et al., 2005; Levinson et al., 2005, 2010). Hemi-synapses can also be induced using microspheres coated with Nlg1, Nrx1 β , or antibodies against Nlg1 or Nrx1 (Dean et al., 2003; Graf et al., 2004; Heine et al., 2008; Barrow et al., 2009), suggesting that the recruitment of scaffolding molecules depends mainly on Nlg1 aggregation.

Other studies have supported more complex mechanisms associated with Nrx1 β /Nlg1 functions. Indeed, synaptic activity is required for Nlg1-mediated stabilization of dendritic filopodia and recruitment of AMPA receptors (Nam and Chen, 2005; Chubykin et al., 2007; Gutiérrez et al., 2009), and for the proteolytic cleavage of Nlg1 (Peixoto et al., 2012). In addition, the postsynaptic interaction between Nlg1 and PSD-95 induces a retrograde modulation of presynaptic release probability (Futai et al., 2007). Thus, besides triggering Nlg1 clustering, Nrx1 β binding to Nlg1 could be associated with signaling mechanisms. One example of ligand-activated adhesion molecules is the integrins, which display a synergy between receptor clustering

and ligand occupancy (Miyamoto et al., 1995), with the latter triggering conformational changes, phosphotyrosine (pY) signaling, and recruitment of actin-associated scaffolds (Giannone and Sheetz, 2006). In neurons, signaling cascades linked to synaptogenic adhesion molecules have been reported (Biederer and Stagi, 2008). EphB receptor engagement of ephrinB causes activation of src family kinases, leading to ephrinB tyrosine phosphorylation and binding to PDZ-domain-containing proteins (Palmer et al., 2002). At the presynapse, Nrxx1 recruits, activates, and is phosphorylated by the CaM kinase CASK, with strong implications for synaptic transmission (Mukherjee et al., 2008). To date, however, no intracellular signaling mechanism associated with Nlg1 has been reported.

Here, we tested the hypothesis that Nrxx1 β binding to Nlg1 can selectively regulate Nlg1's association with scaffolding molecules. We demonstrate that the level of Nlg1 tyrosine phosphorylation at Nrxx1 β /Nlg1 adhesions can trigger the differential recruitment of PSD-95 and gephyrin, thereby potentially controlling the balance between excitatory and inhibitory synapses.

RESULTS

Aggregation of Nlg1 by Nrxx1 β Induces the Rapid Formation of New PSD-95 Clusters

To aggregate Nlg1, we incubated primary rat hippocampal neurons at 6–7 days in vitro (DIV) with purified Nrxx1 β -Fc crosslinked by secondary antibodies (Barrow et al., 2009; Pouloupoulos et al., 2009), and observed the redistribution of Nlg1 and PSD-95 by time-lapse fluorescence microscopy. We previously showed, using Nlg1 knockdown, that Nrxx1 β binds predominantly to Nlg1 (Mondin et al., 2011) and not to other binding partners of Nrxxs, such as Nlg2, Nlg3, or LRRTMs (Graf et al., 2004; de Wit et al., 2009; Pouloupoulos et al., 2009). Here, we confirmed the recruitment of endogenous Nlg1 at Nrxx1 β -Fc clusters (Figure S1A). However, in most experiments, we transfected neurons with Nlg1 and PSD-95 constructs to increase the binding of Nrxxs, such as Nlg2, Nlg3, or LRRTMs (Graf et al., 2004; de Wit et al., 2009; Pouloupoulos et al., 2009). Here, we confirmed the recruitment of endogenous Nlg1 at Nrxx1 β -Fc clusters (Figure S1A). However, in most experiments, we transfected neurons with Nlg1 and PSD-95 constructs to increase the binding of Nrxxs, such as Nlg2, Nlg3, or LRRTMs (Graf et al., 2004; de Wit et al., 2009; Pouloupoulos et al., 2009). Here, we confirmed the recruitment of endogenous Nlg1 at Nrxx1 β -Fc clusters (Figure S1A).

Crosslinked Nrxx1 β induced a rapid coalescence of Nlg1:GFP and PSD-95:GFP from diffuse pools into micron-scale aggregates, matching the size of synapses and colocalizing with Nrxx1 β (Figures 1A and S1B; Movie S1). The number of PSD-95 clusters doubled within 30 min (Figure 1C). This time course is somewhat faster than previously reported time courses (Friedman et al., 2000; Bresler et al., 2001; Barrow et al., 2009; Levinson et al., 2010), possibly owing to different expression levels of Nlg1 and PSD-95. Nevertheless, endogenous PSD-95 was recruited at Nrxx1 β clusters in a time frame similar to that observed for exogenous PSD-95:GFP (Figures 1F and 1G). Whereas soluble Nrxx1 β -Fc inhibits synaptogenesis when used chronically as a competitor of endogenous Nrxx/Nlg interactions (Scheiffele et al., 2000; Levinson et al., 2005; Chen et al., 2010), here acutely added crosslinked Nrxx1 β -Fc mimicked adhesion events that led to the assembly of PSD-95 scaffolds outside pre-existing synapses (Figure S1I).

To ascertain whether PSD-95 was recruited through a specific association with Nlg1, we expressed a C-terminally truncated Nlg1 (Nlg1 Δ Cter) that is unable to bind PSD-95 (Scheiffele

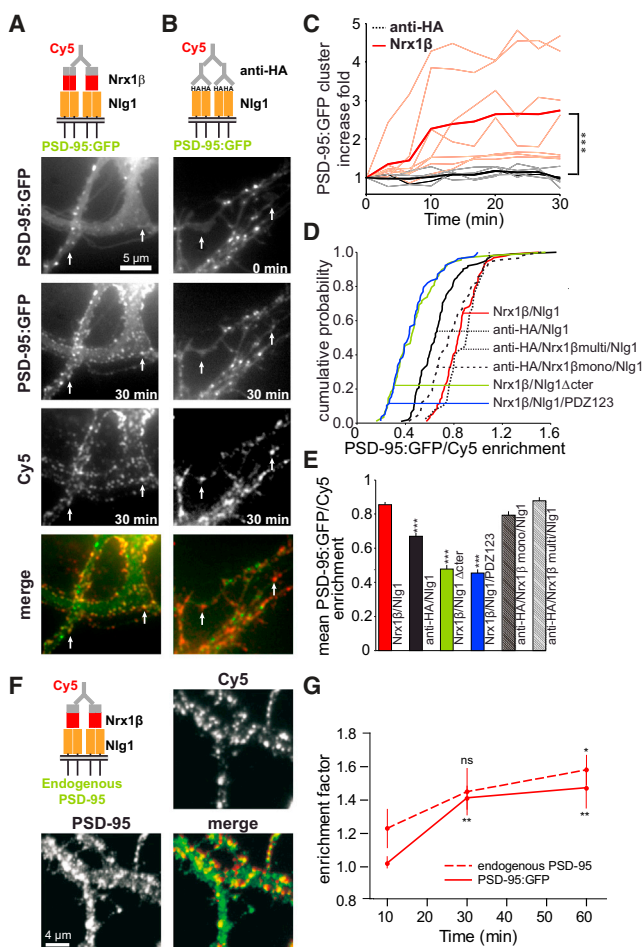


Figure 1. Differential Formation of PSD-95 Clusters by Nrxx1 β -Occupied versus Unoccupied Nlg1

(A and B) Time-course images of PSD-95:GFP (green) in neurons coexpressing HA-Nlg1 and incubated with Nrxx1 β (A) or anti-HA (B), preclustered by Cy5-conjugated secondary antibodies (red).

(C) Kinetics of new PSD-95:GFP cluster formation upon addition of crosslinked Nrxx1 β or anti-HA, normalized by the number of pre-existing PSD-95:GFP clusters. Individual curves are shown (thin lines) together with the average of 5–8 cells (thick lines).

(D) Cumulative distributions of the normalized ratio between PSD-95:GFP and Cy5 enrichments.

(E) Mean \pm SEM of the ratio between PSD-95:GFP and Cy5 enrichment levels for each treatment. Populations were analyzed by one-way ANOVA and compared by Dunn's posttest (** $p < 0.001$).

(F) Neurons expressing Nlg1WT were incubated with crosslinked Nrxx1 β (red) for 1 hr and then immunostained for endogenous PSD-95 (green).

(G) Recruitment kinetics of endogenous PSD-95 (dashed lines) and PSD-95:GFP (plain lines) at Nrxx1 β clusters. The enrichment factor is presented as the mean \pm SEM per cell, and data points were compared with the control 10 min condition by one-way ANOVA, followed by nonparametric Dunn's test (* $p < 0.05$; ** $p < 0.01$).

See also Figures S1 and S2 and Movies S1 and S2.

et al., 2000; Chih et al., 2005). To quantify PSD-95 recruitment at Nrxx1 β /Nlg1 contacts, we calculated a mean PSD-95:GFP enrichment factor and normalized it by the Cy5 signal to correct for cell-to-cell variability in Nlg1 expression level (Figures

S2A–S2C). Despite the efficient formation of $\text{Nrx1}\beta/\text{Nlg1}\Delta\text{Cter}$ contacts, $\text{Nrx1}\beta$ binding to $\text{Nlg1}\Delta\text{Cter}$ was defective in recruiting PSD-95:GFP compared with wild-type Nlg1 (Nlg1WT ; Figures 1D, 1E, and S2C), as reported earlier (Barrow et al., 2009). We obtained a similar result by cotransfecting Nlg1WT and PSD-95:GFP bearing an H-to-V point mutation in each of the three PDZ domains (Schnell et al., 2002) in order to abolish binding to Nlg1 (Figures 1D and 1E). Thus, the recruitment of PSD-95 by Nlg1 aggregates was specific to the PDZ domain-dependent interaction between Nlg1 and PSD-95.

Synergy between Receptor Aggregation and Ligand Occupancy for the Recruitment of PSD-95 by Crosslinked Nlg1

To determine whether $\text{Nrx1}\beta$ binding could stimulate Nlg1 function in addition to increasing its local concentration, we induced Nlg1 aggregation using a “nonactivating” hemagglutinin (HA) antibody directed against an N-terminal HA tag on Nlg1 . This treatment induced a fast and efficient formation of new $\text{Nlg1}:\text{GFP}$ clusters similar to crosslinked $\text{Nrx1}\beta$, with comparable density, size, and Nlg1 content (Figures S1B–S1G). However, very few novel PSD-95:GFP clusters were formed during time-lapse recordings (Figures 1B and 1C; Movie S2). The number of PSD-95 clusters after 30 min induction of Nlg1 aggregation, normalized by the number of pre-existing synaptic clusters, was significantly larger for $\text{Nrx1}\beta$ than for anti-HA (Figure 1C). In addition, PSD-95:GFP enrichment was higher for crosslinked $\text{Nrx1}\beta$ than for anti-HA (Figures 1D and 1E). The difference between $\text{Nrx1}\beta$ and anti-HA in recruiting PSD-95 was not due to the presence of endogenous Nlg1 , because the difference remained in hippocampal cultures from Nlg1 KO mice transfected with Nlg1 (Figures S2D–S2F).

In addition, we measured the recruitment of PSD-95:GFP at Nlg1 aggregates induced by crosslinked anti-HA when soluble $\text{Nrx1}\beta\text{-Fc}$ was added to trigger ligand binding (Figures 1D and 1E). The mean PSD-95:GFP/Cy5 ratio was then similar to that observed at $\text{Nrx1}\beta/\text{Nlg1}$ contacts. Purified $\text{Nrx1}\beta\text{-Fc}$ contained multimeric forms, which could be reduced to monomers by dithiothreitol (DTT) treatment (Figure S1H). The mean PSD-95:GFP/Cy5 ratio upon addition of monomeric $\text{Nrx1}\beta\text{-Fc}$ was also significantly increased compared with crosslinked anti-HA alone (Figures 1D and 1E), ruling out a multimerization effect. Together, these results support the notion that $\text{Nrx1}\beta$ binding not only aggregates Nlg1 but also triggers an additional process that stimulates the $\text{Nlg1}/\text{PSD-95}$ interaction.

Differential PSD-95 Dynamics at Ligand-Occupied or Unoccupied Nlg1 Clusters

To further characterize the potential activation of Nlg1 by $\text{Nrx1}\beta$, we measured the stability of $\text{Nlg1}/\text{PSD-95}$ linkage using fluorescence recovery after photobleaching (FRAP). Newly formed $\text{Nlg1}:\text{GFP}$ or PSD-95:GFP clusters induced by crosslinked $\text{Nrx1}\beta$ or anti-HA were photobleached (Figures 2A and 2B). The recovery rate for $\text{Nlg1}:\text{GFP}$ was similarly low for $\text{Nrx1}\beta$ - and anti-HA-induced clusters (Figure 2C; Table S1), consistent with a robust nanomolar binding affinity between $\text{Nrx1}\beta$ and Nlg1 comparable to that of an antibody (Saint-Michel et al., 2009; Leone et al., 2010). In contrast, the exchange rate for

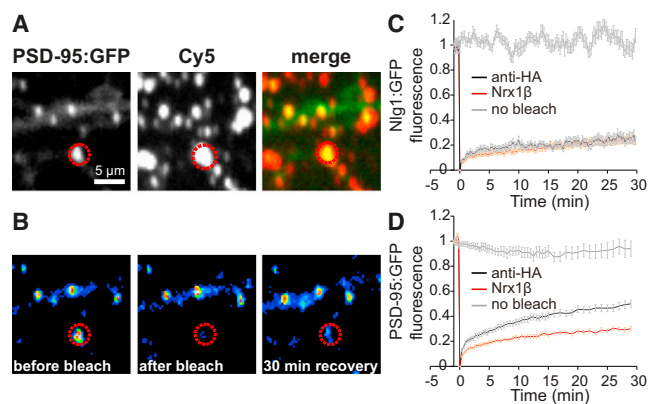


Figure 2. Turnover of Nlg1 and PSD-95 at $\text{Nrx1}\beta$ - or Anti-HA-Induced Clusters

(A) PSD-95:GFP clusters induced by Cy5-labeled crosslinked $\text{Nrx1}\beta$ for 1 hr. (B) FRAP experiment on a PSD-95:GFP cluster (dashed circle). (C) FRAP curves on $\text{Nlg1}:\text{GFP}$ clusters crosslinked by $\text{Nrx1}\beta$ (red) or anti-HA (black). (D) FRAP curves on PSD-95:GFP. Control measurements were made on unbleached $\text{Nlg1}:\text{GFP}$ or PSD-95:GFP clusters (gray curves). Data are presented as the mean \pm SEM of clusters. See also Table S1.

PSD-95 was significantly lower at $\text{Nrx1}\beta/\text{Nlg1}$ adhesions than at anti-HA/ Nlg1 contacts (Figure 2D; Table S1), showing that the interaction between Nlg1 and PSD-95 lasts longer when Nlg1 is bound to $\text{Nrx1}\beta$ than when it is bound to nonactivating antibodies.

Effect of Receptor Occupancy on the Membrane Diffusion of Individual Nlg1 Molecules

To study the effects of ligand binding on the dynamics of $\text{Nlg1}/\text{PSD-95}$ association at synapses, we quantified the membrane diffusion of individual Nlg1 molecules using quantum dots (Qdots) coated with either $\text{Nrx1}\beta\text{-Fc}$ or anti-HA. To label postsynapses, neurons at 10–12 DIV were cotransfected with Homer1c:GFP, which colocalized with PSD-95 (Mondin et al., 2011) without modifying synaptic maturation (Okabe et al., 2001; Heine et al., 2008). Both types of Qdots were very dynamic, oscillating between phases of free diffusion and confinement (Figures 3A and 3B). The distribution of instantaneous diffusion coefficients (Figure 3D) was fitted by two Gaussian curves (Figure S3E), yielding the relative proportions of freely diffusive versus confined events (Figure 3E). Strikingly, the proportion of confined events was 2-fold higher for $\text{Nrx1}\beta$ -coated Qdots (20%) than for anti-HA-coated Qdots (11%; Figures 3D and 3E). The percentage of confined trajectories was increased at the postsynapse (Figures S3A and S3B), suggesting that Nlg1 confinement is triggered through an association with synaptic components. Accordingly, the mean squared displacement (MSD), which reflects the area covered by Nlg1 diffusion, showed a negative curvature consistent with confinement of Nlg1 at synapses (Figure 3F). This behavior was more pronounced for Qdots conjugated to $\text{Nrx1}\beta\text{-Fc}$ than for those conjugated with anti-HA, suggesting a more efficient association with synaptic components. Quantification of the confinement

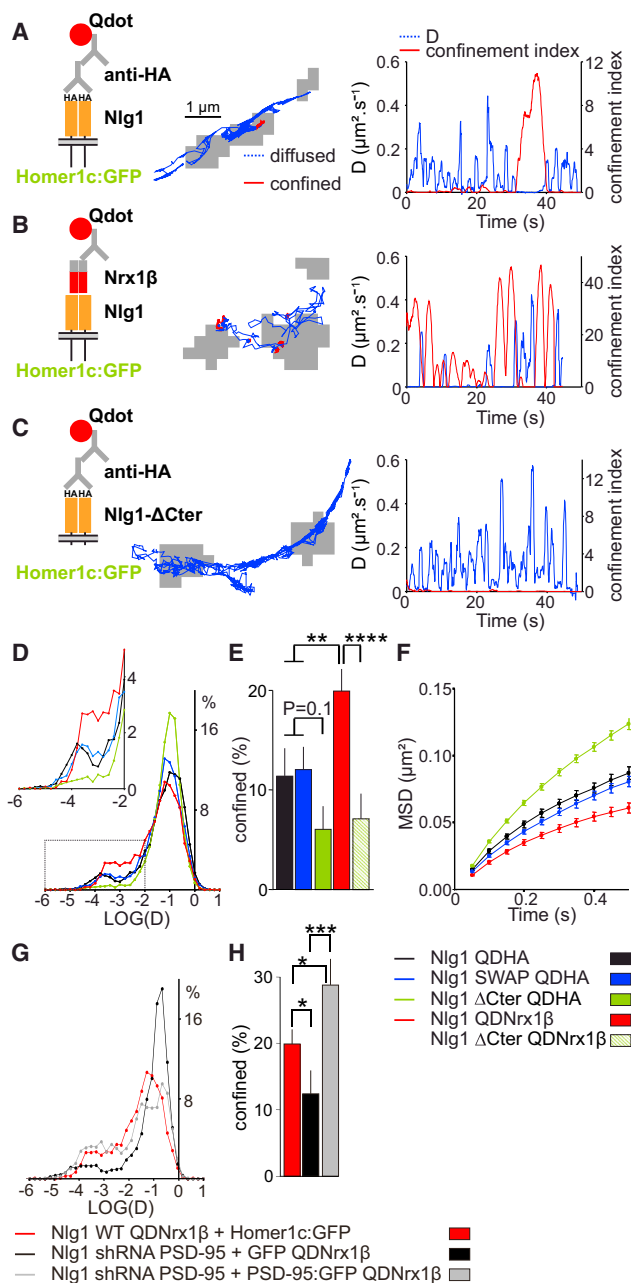


Figure 3. Differential Mobility of Ligand-Occupied versus Unoccupied Nlg1 Molecules Revealed by Single-Nanoparticle Tracking

(A–C) Schematics and representative trajectories of Qdots coated with anti-HA or Nrx1β in neurons expressing Homer1c:GFP (gray pixels), and Nlg1WT or Nlg1ΔCter. Trajectories exhibit both freely diffusive (blue) and confined (red) episodes. Graphs show the corresponding diffusion coefficient (blue) and confinement index (red) over time. A decrease in diffusion coefficient is matched by an increase in confinement index.

(D) Distributions of diffusion coefficients on a logarithmic scale. The confined and freely diffusive events correspond respectively to the leftward and rightward populations fitted by Gaussian curves. Inset: zoom on the distribution of confined events.

(E) Percentage of confined events. The confined fractions obtained by double Gaussian fitting of the distributions were compared by unpaired Student's t tests (**p < 0.01; ****p < 0.0005).

probability for both conditions also demonstrated that ligand-occupied Nlg1 is confined more often than unoccupied Nlg1 (Figure S3F).

The Increased Confinement of Nlg1 Induced by Nrx1β Binding Relies on an Interaction with PSD-95

To determine whether Nlg1 confinement at synapses was due to interactions with intracellular scaffolds or presynaptic Nrxs, we used Nlg1ΔCter, which is unable to bind PSD-95, and an Nlg1SWAP molecule that is unable to bind Nrx1β (Chih et al., 2005; Scheiffele et al., 2000). The confined fraction of anti-HA Qdots bound to Nlg1SWAP was identical to that of Nlg1WT (12%; Figures 3D–3F and S3C), suggesting that Nlg1 confinement is not due to an interaction with presynaptic Nrxs. In contrast, Nlg1ΔCter displayed a reduced fraction of confined events (6%; Figures 3C–3E and S3D). The distribution of diffusion coefficients for Nlg1ΔCter was shifted toward higher values, and the MSD at the postsynapse was almost linear with respect to time, consistent with free diffusion (Figure 3F). When probed with Nrx1β Qdots, Nlg1ΔCter also displayed fewer confined events (7%), suggesting that the increased confinement of Nrx1β-occupied Nlg1 is dependent on its binding to PSD-95 (Figure 3E). Furthermore, knockdown of endogenous PSD-95 expression using small hairpin RNA (shRNA) (Schlüter et al., 2006; Mondin et al., 2011) significantly decreased the confinement of Nrx1β Qdots (13%) compared with control neurons (20%; Figures 3G and 3H). Nlg1 confinement was not totally abolished by shRNA to PSD-95, which might suggest that Nlg1 can bind to other scaffolding proteins, including PSD-93 and S-SCAM, at synapses (Iida et al., 2004). In contrast, when endogenous PSD-95 was replaced by overexpressed PSD-95:GFP, Nlg1 confinement increased to 28% (Figures 3G and 3H). Together, these results strongly support the hypothesis that binding of Nrx1β to Nlg1 stimulates the direct association between Nlg1 and PSD-95.

Nrx1β Binding Rapidly Immobilizes Nlg1

To characterize the dynamics of Nlg1 anchoring to PSD-95 upon ligand binding, we analyzed the diffusion of anti-HA Qdots bound to Nlg1 upon acute addition of soluble Nrx1β (Figures 4A and 4B). Nlg1 molecules were mostly freely diffusive before addition of Nrx1β and became confined freely within 10 min, mostly at Homer1c:GFP locations (Figures 4C and 4D). Accordingly, Nrx1β treatment shifted the diffusion coefficients toward lower values (Figure 4E), an effect that was not observed with the vehicle solution (Figure 4G). Both multimeric and monomeric Nrx1β-Fc induced significant 2.5-fold and 3.1-fold increases in the number of confined events, respectively (Figure 4G). As controls, addition of soluble Nrx1β-Fc multimers on anti-HA Qdots bound to Nlg1SWAP or Nlg1ΔCter, induced modest 1.2-fold and 1.4-fold increases in the number of confined events,

(F) MSD as a function of time at postsynapses.

(G and H) Neurons were cotransfected with Nlg1 plus either shRNA against PSD-95 or a plasmid containing both the shRNA sequence and PSD-95:GFP.

(G) Distributions of diffusion coefficients on a logarithmic scale.

(H) Percentage of confined events (*p < 0.05; ***p < 0.0025).

See also Figure S3.

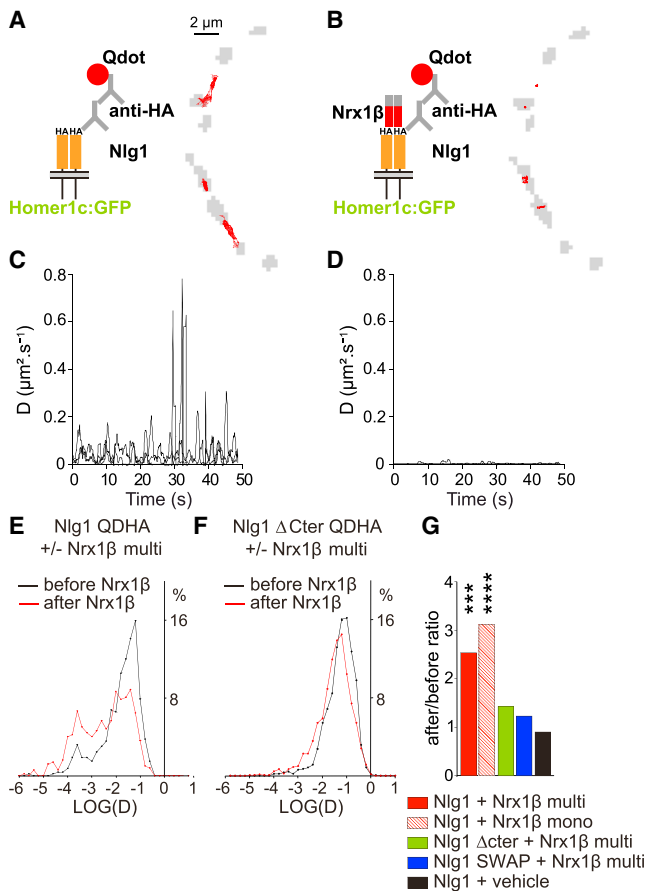


Figure 4. Acute Binding of Soluble Nr1β Quickly Freezes the Lateral Motion of Nlg1 Molecules

(A and B) Schematics and representative trajectories of anti-HA Qdots (red curves) on neurons expressing Homer1c-GFP (gray pixels), acquired before (A) or after 10 min incubation with soluble Nr1β (B). (C and D) Corresponding diffusion coefficients versus time, superimposed for several Qdots. Note the almost zero free diffusion upon Nr1β addition. (E and F) Distributions of diffusion coefficients before (black) and after (red) addition of Nr1β multimers, for Nlg1 WT and Nlg1ΔCter. (G) Ratio of the fractions of confined events, measured after and before addition of Nr1β or vehicle. Confined fractions determined by double Gaussian fitting were compared before and after treatment by paired Student's t test (**p < 0.0025; ****p < 0.001).

respectively (Figures 4F and 4G). These results indicate that the effect of soluble Nr1β-Fc is dependent on a direct binding to Nlg1, and that Nlg1 confinement is due to a rapid anchoring to PSD-95.

Nlg1 Can Be Phosphorylated at Tyrosine 782

By analogy to other adhesion systems (Palmer et al., 2002; Gianone and Sheetz, 2006), we hypothesized that ligand activation of Nlg1 by Nr1β could trigger pY signaling. To examine this hypothesis, we first used broad-spectrum tyrosine kinase and phosphatase inhibitors in the Nr1 cluster assay. The tyrosine kinase inhibitor genistein diminished PSD-95 recruitment level at Nr1β-Fc clusters, whereas the tyrosine phosphatase inhibitor orthovanadate had the opposite effect (Figures 5A and 5B),

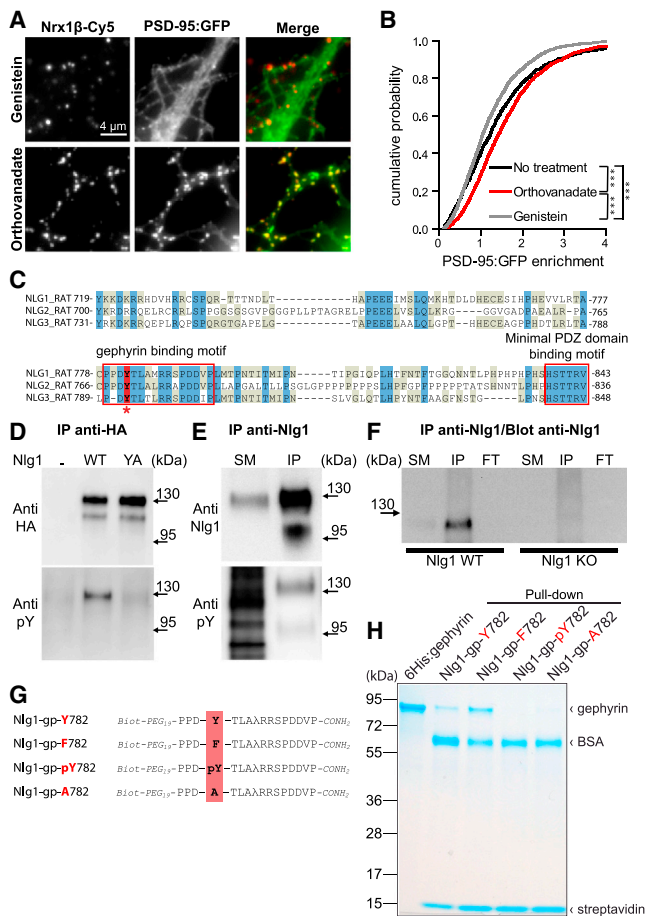


Figure 5. Nlg1 Tyrosine Phosphorylation Controls Direct Binding to Gephyrin

(A and B) Neurons (6–7 DIV) cotransfected with Nlg1 WT and PSD-95:GFP were incubated with crosslinked Nr1β-Fc for 30 min in the presence of 5 μM orthovanadate, 50 μM genistein, or control solution. (A) Representative images. (B) Cumulative distributions of PSD-95:GFP enrichment factor. Populations were analyzed by nonparametric one-way ANOVA and compared by Dunn's posttest. (C) Sequence alignment of the cytoplasmic portion of rat Nlg1, Nlg2, and Nlg3. The conserved gephyrin and PSD-95 PDZ domain-binding motifs are indicated by boxes, and the unique Y782 is shown in red. (D) Extracts of COS cells nontransfected (–) or transfected with Nlg1 WT or Nlg1 YA were immunoprecipitated with anti-HA and immunoblotted for anti-HA or anti-pY. (E) Extracts of neurons (8 DIV) were immunoprecipitated with antibodies to endogenous Nlg1 and immunoblotted with anti-Nlg1 or anti-pY. (F) Brain extracts from WT or Nlg1 KO mice were immunoprecipitated and immunoblotted with anti-Nlg1. FT, flow-through; SM, starting material. (G) Sequences of the biotinylated Nlg1 peptides encompassing the gephyrin-binding motif, with Y782 and modifications highlighted. λ represents Norleucine. (H) Nlg1 peptides immobilized on streptavidin-coated beads were used to pull down recombinant gephyrin in vitro. Samples were run on polyacrylamide gels and Coomassie stained. The three bands correspond to 6His:gephyrin (82 kDa), BSA (69 kDa) to reduce nonspecific binding, and streptavidin (13 kDa) to control sample loading. See also Table S2.

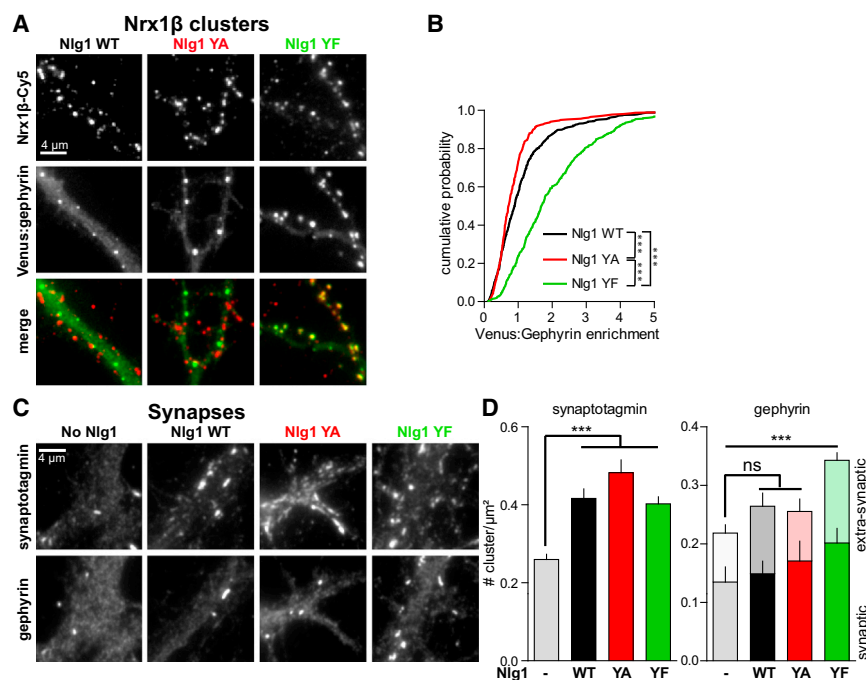


Figure 6. Recruitment of Gephyrin by Nlg1 Tyrosine Point Mutants in Cluster and Synapse Induction Assays

(A) Neurons (8 DIV) cotransfected with Venus:gephyrin plus Nlg1WT, Nlg1YA, or Nlg1YF were incubated with crosslinked Nrx1 β -Fc.

(B) Cumulative distributions of the Venus:gephyrin enrichment factor at Nrx1 β -Fc clusters. Populations were analyzed by nonparametric one-way ANOVA and compared by Dunn's posttest (** $p < 0.001$).

(C) Neurons (9–10 DIV) transfected with GFP alone or cotransfected with GFP plus Nlg1WT or Nlg1 point mutants were immunostained for endogenous synaptotagmin and gephyrin.

(D) Numbers of synaptotagmin or gephyrin puncta per dendrite area (mean \pm SEM). Lower bars represent gephyrin puncta opposed to synaptotagmin puncta, and upper bars correspond to extrasynaptic gephyrin puncta. Populations were analyzed by parametric one-way ANOVA and Bonferroni's posttest (** $p < 0.001$; ns, not significant).

See also Figures S4 and S5.

indicating that tyrosine phosphorylation is implicated in PSD-95 binding to Nlg1. Although these agents can affect the tyrosine phosphorylation of many proteins, a phospho-proteomic screen of tyrosine-phosphorylated peptides in cancer cells identified a sequence corresponding to Nlg1 (Rikova et al., 2007), suggesting that Nlg1 itself can be tyrosine phosphorylated. In fact, there is a unique tyrosine located in the middle of the Nlg1 intracellular domain (Y782; Figure 5C). To demonstrate that this tyrosine could be phosphorylated, we performed pY immunoblots on immunoprecipitated Nlg1. Nlg1 transfected in COS cells and immunoprecipitated with anti-HA was tyrosine phosphorylated, as revealed by a band at 130 kDa (Figure 5D), corresponding to the apparent Nlg1 molecular weight (Dean et al., 2003). The pY signal was not observed in untransfected cells or in COS cells transfected with an Nlg1 point mutant in which this tyrosine was replaced by alanine (Nlg1YA), demonstrating that Y782 was the only phosphorylated tyrosine in Nlg1. We also immunoprecipitated endogenous Nlg1 from rat hippocampal neurons, and detected a pY band at the Nlg1 apparent molecular weight (Figure 5E), showing that Nlg1 was tyrosine phosphorylated in neurons. We checked the specificity of the Nlg1 antibody by performing immunoprecipitation (IP) on brain extracts from WT mice compared with *Nlg1* KO littermates (Figure 5F). These results strongly indicated that Nlg1 can be phosphorylated at position Y782.

The Phosphorylation State of Y782 in Nlg1 Peptides Regulates Gephyrin Binding In Vitro

Y782 is a unique tyrosine that belongs to a consensus region that is conserved among all Nlgs. It is critical for binding to gephyrin (Figure 5C), a major scaffold at inhibitory synapses (Poulopoulos et al., 2009). Specifically, a Y770A mutation in Nlg2 was shown to prevent binding to gephyrin (Poulopoulos et al., 2009). To assess

whether the phosphorylation of Y782 in Nlg1 affected gephyrin binding, we generated peptides encompassing the gephyrin-binding motif and performed in vitro pull-down of recombinant gephyrin. We designed four peptides (Figure 5G): (1) Nlg1-gp-Y782, containing the nonmodified tyrosine; (2) Nlg1-gp-pY782, containing the phosphorylated tyrosine; (3) Nlg1-gp-A782, where the tyrosine was replaced by an alanine; and (4) Nlg1-gp-F782, where the tyrosine was replaced by a phenylalanine, preserving the aromatic ring and mimicking the structure of an unphosphorylated tyrosine. Gephyrin was pulled down very efficiently by both the Nlg1-gp-Y782 and Nlg1-gp-F782 peptides (Figure 5H), indicating that gephyrin binds the nonphosphorylated form of Nlgs. In contrast, gephyrin could not be pulled down by either the Nlg1-gp-pY782 or Nlg1-gp-A782 peptide, indicating that gephyrin cannot bind the phosphorylated form of Nlgs, most likely because the binding site does not tolerate a bulky negatively charged phosphate group. Thus, with respect to gephyrin binding, the Y-to-A mutation produces the same effect as phosphorylated Nlg1, whereas the Y-to-F mutation shows the same effect as the constitutively unphosphorylated Nlg1. We therefore generated two Nlg1 mutants (Y782F and Y782A) that will either bind or not bind to gephyrin, thus mimicking the effect of nonphosphorylated and phosphorylated Nlg1, respectively.

Nlg1 Y782 Point Mutants Regulate Gephyrin Recruitment and Inhibitory Synapse Formation in Neurons

To examine whether the binding of Nlg1 to gephyrin was controlled by tyrosine phosphorylation in neurons, we expressed Nlg1 tyrosine point mutants and characterized the recruitment of Venus:gephyrin at Nrx1 β clusters (Figures 6A and 6B). The densities of Nrx1 β clusters on neurons expressing Nlg1 mutants

or Nlg1WT were similar, showing that Nlg1 mutants were expressed at the cell surface and bound to Nrx1 β (Figure S4A). In this assay, exogenous Nlg1 mutants outnumbered endogenous Nlg1 and Nlg3 (Mondin et al., 2011), with which they can potentially oligomerize (Pouloupoulos et al., 2012), thus enabling us to assess the effects of those mutations. The enrichment of Venus:gephyrin was slightly but significantly lower for Nlg1YA than for Nlg1WT, suggesting that Nlg1WT partly associates with gephyrin, and that Nlg1 tyrosine phosphorylation inhibits this interaction. Strikingly, the enrichment of Venus:gephyrin was much higher for Nlg1YF than for Nlg1WT, confirming the *in vitro* data and supporting the notion that unphosphorylated Nlg1 strongly binds gephyrin.

Although Nlg1 is mostly associated with PSD-95 at excitatory synapses, previous studies showed that a fraction of endogenous Nlg1 (20%) associates with inhibitory synapses (Levinson et al., 2005, 2010) and coimmunoprecipitates with gephyrin (Varley et al., 2011). Using immunocytochemistry in untransfected neurons, we confirmed that endogenous Nlg1 was preferentially recruited at PSD-95 puncta and also significantly recruited at gephyrin puncta (Figure S5). To characterize the role of Nlg1 phosphorylation on inhibitory synapse formation, we examined the distribution of endogenous gephyrin in neurons transfected with Nlg1 mutants. Both extrasynaptic and synaptic puncta apposed to presynaptic terminals counterstained for synaptotagmin were quantified. Expression of Nlg1WT, Nlg1YA, and Nlg1YF doubled the number of presynapses that formed on transfected neurons compared with untransfected cells (Figures 6C and 6D), a classical effect induced by Nlg1 overexpression. Neurons transfected with Nlg1WT and Nlg1YA contained slightly more gephyrin puncta, in agreement with reports showing that Nlg1 overexpression increases the numbers of both excitatory and inhibitory synapses (Chih et al., 2005, 2006; Levinson et al., 2005; Ko et al., 2009). In contrast, the Nlg1YF mutant strongly increased the density of both synaptic and extrasynaptic gephyrin puncta compared with Nlg1WT and Nlg1YA, suggesting that nonphosphorylated Nlg1 stimulates the formation of inhibitory synapses.

Nlg1 Y782 Point Mutants Regulate PSD-95 Recruitment and Excitatory Synapse Formation in Neurons

We then hypothesized that binding of gephyrin to Nlg1, regulated by tyrosine phosphorylation, might affect the interaction between PSD-95 and the Nlg1 C terminus (Irie et al., 1997; Figure 5C). We expressed Nlg1 point mutants in neurons and examined the recruitment of PSD-95 in both cluster and synapse induction assays. The effects found with PSD-95 exactly mirrored those observed with gephyrin. Specifically, PSD-95:GFP enrichment at Nrx1 β clusters was significantly higher in neurons transfected with Nlg1YA and Nlg1WT compared with Nlg1YF (Figures 7A and 7B). Since the YA and YF mutations mimic the effects of constitutively phosphorylated and unphosphorylated Nlg1, respectively, these results support the notion that phosphorylation of Y782 enhanced Nlg1 binding to PSD-95.

When Nlg1WT was aggregated with anti-HA clusters, PSD-95:GFP recruitment was lower than that observed with Nrx1 β clusters (Figures 1, 7C, and 7D). The PSD-95 recruitment level induced by Nlg1WT was as low as that obtained with the Nlg1YF

mutant (Figures 7B and 7D), suggesting that aggregation of Nlg1 without ligand binding is associated with unphosphorylated Nlg1. In contrast, PSD-95:GFP recruitment at anti-HA clusters was significantly higher for Nlg1YA (Figure 7D), reaching the levels obtained with Nlg1WT at Nrx1 β clusters (Figure 7B) and supporting the view that the Nlg1YA mutant bypassed Nrx-dependent signaling by mimicking the effect of constitutive phosphorylation of Nlg1. These effects could not be attributed to differences in surface expression or clustering of Nlg1 point mutants, because the density of anti-HA clusters was similar to that of Nlg1WT (Figure S4). These data suggest that in the absence of Nrx1 β binding, Nlg1 is unphosphorylated and binds PSD-95 less efficiently, whereas upon Nrx1 β binding, Nlg1 is phosphorylated and recruits PSD-95.

To characterize the role of the Nlg1 phosphorylation state in excitatory synapse formation, we quantified the number of synaptic and extrasynaptic puncta of endogenous PSD-95 in neurons transfected with Nlg1 point mutants. Both Nlg1WT and Nlg1YA doubled the density of both synaptic and extrasynaptic PSD-95 puncta (Figures 7E and 7F). In contrast, neurons transfected with Nlg1YF had a similarly low PSD-95 cluster density compared with cells expressing GFP alone. The striking difference between Nlg1WT and Nlg1YA versus Nlg1YF in terms of the density of endogenous PSD-95 puncta indicates that Nlg1 tyrosine phosphorylation selectively triggers excitatory synapse formation. The comparable effects of Nlg1 tyrosine mutations on PSD-95 recruitment at endogenous synapses and Nrx1 β clusters suggest that Nrx1 β was the presynaptic ligand for Nlg1 in the synapse induction assay. This is consistent with studies showing that chronic incubation with soluble Nrx1 β inhibits *de novo* synapse formation (Levinson et al., 2005; Chih et al., 2006; Chen et al., 2010). Finally, the fact that both Nlg1WT and Nlg1YA preferentially recruited PSD-95 versus gephyrin in Nrx1 β clusters and synapse induction assays indicates that Nrx1 β -occupied Nlg1 at transsynaptic adhesions is likely to be tyrosine phosphorylated.

DISCUSSION

This study shows that Nrx1 β adhesion to Nlg1 promotes a fast and direct interaction between Nlg1 and PSD-95, not only through receptor clustering but also through a specific ligand-binding effect linked to pY signaling. Thus, similarly to integrins (Miyamoto et al., 1995; Giannone and Sheetz, 2006) and ephrins (Palmer et al., 2002; Biederer and Stagi, 2008), Nlg1 can be considered as a ligand-activated adhesion molecule. Our data support a competitive model in which unoccupied tyrosine-unphosphorylated Nlg1 binds more to gephyrin, preventing PSD-95 accessibility, whereas ligand-occupied phosphorylated Nlg1 interacts less with gephyrin and is accessible to PSD-95 binding (Figure S6). This process may play an important role in regulating the balance between excitatory and inhibitory synapse formation.

Nrx1 β Binding Enhances PSD-95 Recruitment Compared with Nlg1 Multimerization Alone

We have revealed that individual Nlg1 molecules alternate between free diffusion and confinement at the neuronal

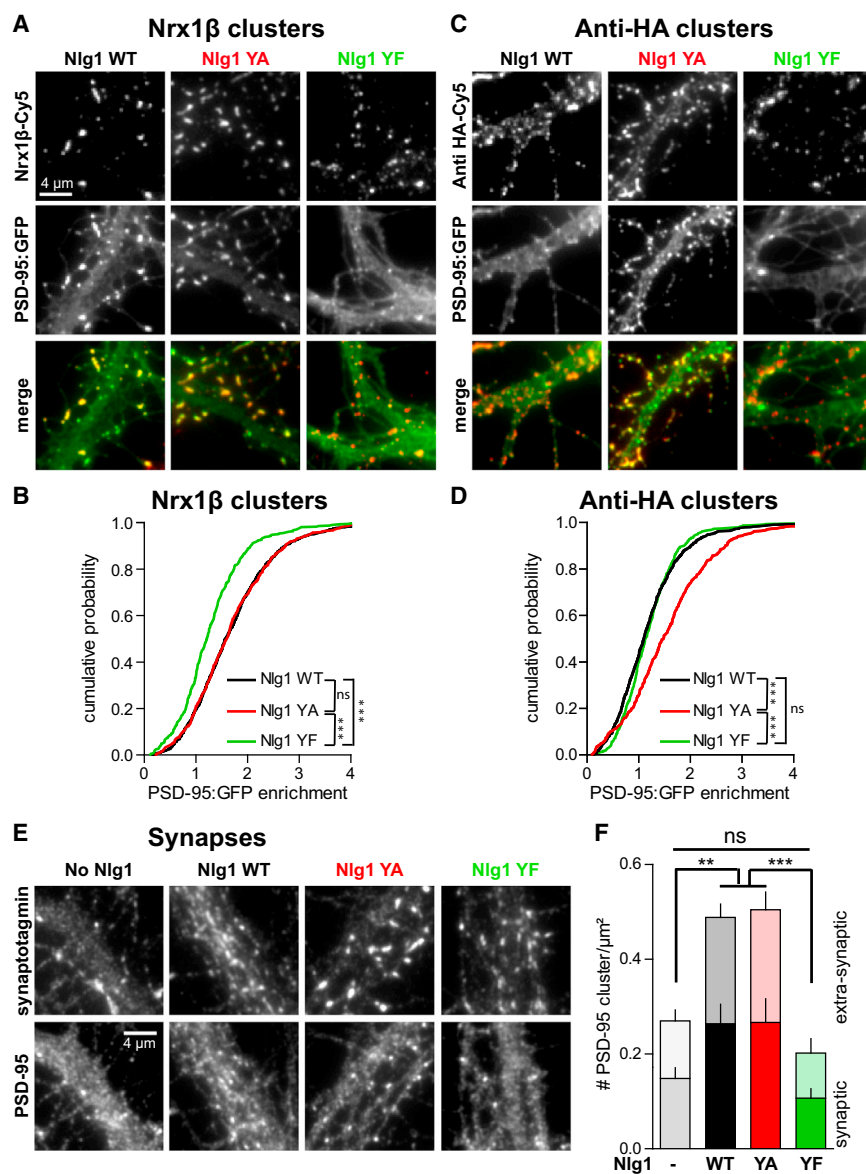


Figure 7. Recruitment of PSD-95 by Nlg1 Tyrosine Point Mutants in Cluster and Synapse Induction Assays

(A and C) Neurons (6–7 DIV) cotransfected with PSD-95:GFP plus Nlg1WT or Nlg1 point mutants were incubated with crosslinked Nrx1β-Fc or anti-HA.

(B and D) Cumulative distributions of the PSD-95:GFP enrichment factor. Populations were analyzed by nonparametric one-way ANOVA and compared by Dunn’s posttest (** $p < 0.001$; ns, not significant).

(E) Neurons (8–10 DIV) transfected with GFP alone or cotransfected with GFP plus Nlg1WT or Nlg1 point mutants were immunostained for endogenous synaptotagmin and PSD-95.

(F) Numbers of PSD-95 puncta per dendrite area (mean \pm SEM). Lower bars represent PSD-95 puncta opposed to synaptotagmin puncta, and upper bars correspond to extrasynaptic PSD-95 puncta. Populations were analyzed by parametric one-way ANOVA and Bonferroni’s posttest (** $p < 0.001$).

See also Figure S6.

(Schlüter et al., 2006) may allow the formation of a platform of multivalent binding sites for unoccupied diffusive Nlg1 dimers (Dean et al., 2003; Pouloupoulos et al., 2012).

However, compared with HA antibodies, Nrx1β ligands induced (1) an increased probability of association between Nlg1 and PSD-95 in single-particle tracking, (2) a faster assembly of PSD-95 clusters and stronger recruitment of PSD-95 in crosslinking assays, and (3) a more stable Nlg1/PSD-95 interaction in FRAP experiments. Remarkably, the acute addition of soluble Nrx1β to Nlg1 aggregated by HA antibodies in both the cluster and Qdot assays provided direct

surface. Nlg1 trapping occurred both in the extrasynaptic space and at synapses through binding to scaffolding molecules, including PSD-95. In addition to the transport of preformed postsynaptic packets (Gerrow et al., 2006; Barrow et al., 2009; Gutiérrez et al., 2009), this diffusion/trapping mechanism could represent an efficient way to rapidly regulate the numbers of Nlg1 at nascent or mature synaptic contacts (Mondin et al., 2011). The aggregation of Nlg1 by HA antibodies showed significant recruitment of PSD-95 compared with the control Nlg1ΔCter. This result is consistent with the finding that PSD-95 recruitment can be induced by aggregating Nlg1 (Graf et al., 2004; Barrow et al., 2009). Furthermore, anti-HA-conjugated Qdots bound to Nlg1WT or Nlg1SWAP occasionally stuck to synapses, indicating a basal level of interaction between Nlg1 and PSD-95 even in the absence of ligand binding. The dimerization of PSD-95

evidence that Nrx1β binding changed the association state between Nlg1 and PSD-95.

Tyrosine Phosphorylation of Nlg1 Controls the Differential Recruitment of Gephyrin and PSD-95

There is a strong sequence homology among Nlg1s in both the gephyrin and the C-terminal PSD-95 binding motifs, and both Nlg1 and Nlg2 are capable of binding to either PSD-95 or gephyrin (Irie et al., 1997; Graf et al., 2004; Pouloupoulos et al., 2009). Previous experiments showed that an Nlg2 truncation mutant ($\Delta 716-782$) lacking the gephyrin-binding motif was delocalized from inhibitory synapses (Levinson et al., 2010). Furthermore, Pouloupoulos et al. (2009) showed that an Nlg2Y770A mutant was unable to bind recombinant gephyrin in vitro and recruited less endogenous gephyrin than Nlg2WT. The authors indicated that this tyrosine is essential for gephyrin binding, but did not explore whether

its potential phosphorylation regulates gephyrin binding. Our experiments *in vitro* and in neurons clearly show that phosphorylation of this tyrosine prevents direct gephyrin binding and favors interaction with PSD-95. These data suggest a competition between gephyrin and PSD-95 for binding to the intracellular tail of Nlg, regulated by ligand binding and the phosphorylation level. A similar pY switch was previously proposed for the competitive binding of talin and tensin to the C-terminal tail of integrins (Legate and Fässler, 2009), and binding of ankyrin to the adhesion molecule L1 (Gil et al., 2003). Because the distance between the gephyrin-binding sequence and the C-terminal PSD-95 binding motif is relatively short (43 aa), and both gephyrin and PSD-95 can form multimers (Schlüter et al., 2006; Saiyed et al., 2007), a steric hindrance or binding motif sequestering could explain the competitive binding between those proteins. Previous studies demonstrated a sequestering mechanism for the binding of PSD-95 to stargazin in neurons, whereby stargazin interacts in a phosphorylation-dependent manner to negatively charged lipid bilayers, preventing access to PSD-95 PDZ domains (Opazo et al., 2010; Sumioka et al., 2010).

Implications of Nlg pY Signaling in Synapse Development

The balance between excitatory and inhibitory synapse formation mediated by Nlgs was previously shown to be bidirectionally controlled by the expression levels of PSD-95 and gephyrin (Chih et al., 2005; Levinson et al., 2005, 2010). These results indicated that controlling the strength of association of PSD-95 or gephyrin to Nlgs could determine the respective numbers of excitatory versus inhibitory synapses. Our results with Nlg1 point mutants strongly suggest that the level of Nlg1 tyrosine phosphorylation controls this balance. Specifically, the ratio between excitatory versus inhibitory synapse numbers was high (1.8) for Nlg1YA mimicking phosphorylated Nlg1, and low (0.6) for Nlg1YF mimicking unphosphorylated Nlg1. Such a regulation of the pY level might be relevant for other Nlgs, in particular Nlg3, which can associate with both excitatory and inhibitory synapses (Levinson et al., 2010; Shipman et al., 2011) and form heterodimers with Nlg1 (Poulopoulos et al., 2012). The specific localization of the different Nlgs to either excitatory or inhibitory synapses may also be regulated by additional intracellular binding partners. For example, Nlg1/3-mediated excitatory synaptic transmission is controlled by a noncanonical sequence situated upstream of the gephyrin binding motif (Shipman et al., 2011). Moreover, Nlg2 bears a specific motif (absent in Nlg1 and Nlg3) that activates collybistin, bringing gephyrin to the cell surface and favoring its association with Nlg2 at inhibitory synapses (Varoqueaux et al., 2004; Poulopoulos et al., 2009). Yet, the strong recruitment of gephyrin by the Nlg1Y782F mutant lacking the collybistin interaction motif suggests that a direct interaction with collybistin is not required for gephyrin recruitment by Nlg1.

Such a ligand-induced pY “switch” could represent a very sensitive mechanism in synaptogenesis, during which early neuronal contacts that rely on Nrx/Nlg adhesion may be primed to assemble functional excitatory or inhibitory postsynapses. PSD-95 recruited by Nrx/Nlg adhesions may serve as a scaffold

for the trapping of surface-diffusing AMPA receptors (Heine et al., 2008; Mondin et al., 2011), whereas the recruitment of NMDA receptors may occur through a direct interaction with Nlg1 (Budreck et al., 2013). Gephyrin could play the same role at nascent inhibitory synapses by trapping glycine and GABA receptors (Meier et al., 2001; Bannai et al., 2009). The phosphorylation level of Nlgs may be implicated not only in synapse formation but also in later stages of synapse stabilization and plasticity. Indeed, synaptic activity is required for Nlg-dependent synapse validation (Nam and Chen, 2005; Chubykin et al., 2007) and for the stabilization of PSD-95 at synapses (Mondin et al., 2011). Given the intrinsic turnover of scaffolding molecules at synapses (Okabe et al., 1999; Sturgill et al., 2009), it is possible that the recurrent phosphorylation or dephosphorylation of Nlgs is involved in retaining PSD-95 and gephyrin at mature excitatory and inhibitory synapses, respectively.

Control of the Local pY Signaling Mechanism

Although our results indicate that ligand binding to Nlg1 favors tyrosine phosphorylation, at this stage we do not know which kinases or phosphatases are involved. Interestingly, Nrx/Nlg adhesions interact with a pY phosphatase receptor (PTPRT) that has been implicated in glutamatergic synapse development and whose activity is regulated by the Fyn tyrosine kinase (Lim et al., 2009). However, it is still unclear whether Nlgs can be directly phosphorylated by Fyn and/or dephosphorylated by PTPRT. Another candidate is the neurotrophin receptor tyrosine kinase TrkC, which has been shown to mediate excitatory post-synaptic formation (Takahashi et al., 2011). One possibility is that different sets of tyrosine kinases and phosphatases are recruited in excitatory versus inhibitory synapses, leading to differential phosphorylation of Nlg1.

Interestingly, Nrxs and Nlgs exist as many different isoforms and splice variants, giving rise to a variety of structural interfaces and affinities, and precise associations between these Nrx and Nlg variants contribute to the specification of synapses (Craig and Kang, 2007; Südhof, 2008). Specifically, addition of the S4 insert in Nrx1 β selectively reduces its ability to bind Nlg1 and recruit PSD-95, but has little effect on binding to Nlg2 and recruitment of gephyrin (Graf et al., 2006). On the other hand, inclusion of a splice insertion at site B in Nlg1 and Nlg2 promotes the formation of excitatory rather than inhibitory synapses (Chih et al., 2006). One exciting possibility is that certain combinations of Nrx/Nlg isoforms and splice variants promote Nlg tyrosine phosphorylation, favoring excitatory synapse formation, whereas other combinations prevent Nlg tyrosine phosphorylation, inducing inhibitory synapses. Finally, since pathological mutations in Nlgs are associated with autism and mental retardation in humans (Südhof, 2008), pharmacological compounds directed toward the Nlg-specific tyrosine kinase/phosphatase pathway, allowing regulation of the excitation/inhibition balance, may provide therapeutic treatments for these disorders.

EXPERIMENTAL PROCEDURES

Cell Culture

For cluster assays, single-particle experiments, and immunocytochemistry, dissociated embryonic day 18 (E18) rat hippocampal neurons were cultured

on glass coverslips on top of a feeder layer of astrocytes. Two days before experiments were conducted, neurons were transfected by lipofection with various Nlg1, PSD-95, gephyrin, or Homer1c constructs. For biochemistry, untransfected rat neuronal cultures or COS cells transfected with Nlg1 constructs were lysed, followed by anti-HA or anti-Nlg1 IP and western blotting. In some experiments, whole-brain extracts or dissociated neuronal cultures were prepared from Nlg1WT or *Nlg1* KO mice.

Cluster Assays

Purified Nr1 β -Fc or HA antibodies were crosslinked by Cy5-conjugated anti-human Fc or anti-rat Fc antibodies, respectively, and added to neurons for 30 min to 1 hr at 37°C. Neurons were either observed live or immunostained for Nlg1, PSD-95, gephyrin, or synapsin. In some experiments, multimeric or monomeric soluble Nr1 β -Fc was added to neurons during incubation with crosslinked HA antibodies.

FRAP

Nlg1:GFP and PSD-95:GFP clusters were formed for 1 hr as described above and photobleached using an inverted microscope equipped with a spinning disk confocal system and a multispot FRAP setup. Fluorescence recovery was recorded for 30 min.

Single-Particle Tracking Experiments

Neurons cotransfected with Homer1c:GFP and various Nlg1 constructs were incubated with 655 nm Qdots conjugated with either Nr1 β -Fc or HA antibodies, and imaged at 20 Hz on an inverted epifluorescence microscope equipped with an EMCCD camera. In some experiments, soluble Nr1 β -Fc was added live on neurons labeled with anti-HA-coated Qdots. Images were analyzed by a segmentation and tracking program written within Metamorph (Mondin et al., 2011).

Pull-Down of Gephyrin by Nlg1 Peptides

Biotinylated Nlg1 peptides encompassing the gephyrin-binding motif were synthesized by standard solid-phase methods, purified by reversed-phase high-performance liquid chromatography (RP-HPLC), and characterized by RP-HPLC and MALDI-TOF. Streptavidin-coated beads saturated with peptides were incubated with recombinant gephyrin in the presence of BSA. Proteins recovered by boiling the beads were separated by SDS-PAGE and Coomassie stained.

IP and Western Blotting

COS cells, mixed neuronal cultures, or mice brains were scraped off in lysis buffer containing phosphatase inhibitors and nonionic detergents. Nlg1 was immunoprecipitated from these samples using protein-G-coated magnetic beads and HA (for COS cells) or Nlg1 antibodies (for neurons or brain extracts). Beads were boiled in sample buffer and recovered proteins were separated by SDS-PAGE, transferred to nitrocellulose membranes, and processed for immunoblotting using HA, Nlg1, or pY antibodies. Immunoreactive bands were revealed by horseradish peroxidase and chemiluminescence.

Statistics

The numbers of cells, clusters, Qdot trajectories, and synaptic puncta examined in all conditions are given in [Extended Experimental Procedures](#). The statistical tests described in the figure legends refer to these populations.

SUPPLEMENTAL INFORMATION

Supplemental Information includes Extended Experimental Procedures, six figures, two tables, and two movies and can be found with this article online at <http://dx.doi.org/10.1016/j.celrep.2013.05.013>.

LICENSING INFORMATION

This is an open-access article distributed under the terms of the Creative Commons Attribution License, which permits unrestricted use, distribution,

and reproduction in any medium, provided the original author and source are credited.

ACKNOWLEDGMENTS

We thank P. Scheiffele, H. Betz, O. Schlüter, S. Okabe, N. Brose, C. Dotti, and A. Triller for the generous gifts of reagents and animals. We thank C. Breillat, A. Frouin, D. Bouchet, and N. Retailleau for cell culture; P. Gonzales and R. Sterling for technical assistance; A. Gautreau and F. Coussen for help with biochemistry; and M. Heine, X. Fournet, and I. Gauthereau for experimental contributions. We thank C. Poujol and P. Legros at the Bordeaux Imaging Center for help with FRAP experiments and image analysis, the Genomic Transcriptomic Facility of Bordeaux for DNA sequencing, and the Proteomics Platform of the Bordeaux Center for Functional Genomics for peptide analysis. The research leading to these results was funded by the European Union's Seventh Framework Program under grant agreement 232942 Nano-Dyn-Syn, the Centre National de la Recherche Scientifique, the Agence Nationale pour la Recherche (grants Neurologion, Synapse-2Dt, and ChemTraffic), a Marie Curie Intra-European Fellowship (neuroCHEMbiotools), the Conseil Régional Aquitaine, and the Fondation pour la Recherche Médicale.

Received: August 14, 2012

Revised: March 8, 2013

Accepted: May 9, 2013

Published: June 13, 2013

REFERENCES

- Bannai, H., Lévi, S., Schweizer, C., Inoue, T., Launey, T., Racine, V., Sibarita, J.-B., Mikoshiba, K., and Triller, A. (2009). Activity-dependent tuning of inhibitory neurotransmission based on GABAAR diffusion dynamics. *Neuron* 62, 670–682.
- Barrow, S.L., Constable, J.R., Clark, E., El-Sabeawy, F., McAllister, A.K., and Washbourne, P. (2009). Neuroligin1: a cell adhesion molecule that recruits PSD-95 and NMDA receptors by distinct mechanisms during synaptogenesis. *Neural Dev.* 4, 17.
- Biederer, T., and Stagi, M. (2008). Signaling by synaptogenic molecules. *Curr. Opin. Neurobiol.* 18, 261–269.
- Bresler, T., Ramati, Y., Zamorano, P.L., Zhai, R., Garner, C.C., and Ziv, N.E. (2001). The dynamics of SAP90/PSD-95 recruitment to new synaptic junctions. *Mol. Cell. Neurosci.* 18, 149–167.
- Budreck, E.C., Kwon, O.-B., Jung, J.H., Baudouin, S., Thommen, A., Kim, H.-S., Fukazawa, Y., Harada, H., Tabuchi, K., Shigemoto, R., et al. (2013). Neuroligin-1 controls synaptic abundance of NMDA-type glutamate receptors through extracellular coupling. *Proc. Natl. Acad. Sci. USA* 110, 725–730.
- Chen, S.X., Tari, P.K., She, K., and Haas, K. (2010). Neurexin-neuroligin cell adhesion complexes contribute to synaptotropic dendritogenesis via growth stabilization mechanisms in vivo. *Neuron* 67, 967–983.
- Chih, B., Engelman, H., and Scheiffele, P. (2005). Control of excitatory and inhibitory synapse formation by neuroligins. *Science* 307, 1324–1328.
- Chih, B., Gollan, L., and Scheiffele, P. (2006). Alternative splicing controls selective trans-synaptic interactions of the neuroligin-neurexin complex. *Neuron* 51, 171–178.
- Chubykin, A.A., Atasoy, D., Etherton, M.R., Brose, N., Kavalali, E.T., Gibson, J.R., and Südhof, T.C. (2007). Activity-dependent validation of excitatory versus inhibitory synapses by neuroligin-1 versus neuroligin-2. *Neuron* 54, 919–931.
- Craig, A.M., and Kang, Y. (2007). Neurexin-neuroligin signaling in synapse development. *Curr. Opin. Neurobiol.* 17, 43–52.
- de Wit, J., Sylwestrak, E., O'Sullivan, M.L., Otto, S., Tiglio, K., Savas, J.N., Yates, J.R., 3rd, Comoletti, D., Taylor, P., and Ghosh, A. (2009). LRRTM2 interacts with Neurexin1 and regulates excitatory synapse formation. *Neuron* 64, 799–806.

- Dean, C., Scholl, F.G., Choih, J., DeMaria, S., Berger, J., Isacoff, E., and Scheiffele, P. (2003). Neurexin mediates the assembly of presynaptic terminals. *Nat. Neurosci.* *6*, 708–716.
- Friedman, H.V., Bresler, T., Garner, C.C., and Ziv, N.E. (2000). Assembly of new individual excitatory synapses: time course and temporal order of synaptic molecule recruitment. *Neuron* *27*, 57–69.
- Futai, K., Kim, M.J., Hashikawa, T., Scheiffele, P., Sheng, M., and Hayashi, Y. (2007). Retrograde modulation of presynaptic release probability through signaling mediated by PSD-95-neuroigin. *Nat. Neurosci.* *10*, 186–195.
- Gerrow, K., Romorini, S., Nabi, S.M., Colicos, M.A., Sala, C., and El-Husseini, A. (2006). A preformed complex of postsynaptic proteins is involved in excitatory synapse development. *Neuron* *49*, 547–562.
- Giannone, G., and Sheetz, M.P. (2006). Substrate rigidity and force define form through tyrosine phosphatase and kinase pathways. *Trends Cell Biol.* *16*, 213–223.
- Gil, O.D., Sakurai, T., Bradley, A.E., Fink, M.Y., Cassella, M.R., Kuo, J.A., and Felsenfeld, D.P. (2003). Ankyrin binding mediates L1CAM interactions with static components of the cytoskeleton and inhibits retrograde movement of L1CAM on the cell surface. *J. Cell Biol.* *162*, 719–730.
- Graf, E.R., Zhang, X., Jin, S.-X., Linhoff, M.W., and Craig, A.M. (2004). Neurexins induce differentiation of GABA and glutamate postsynaptic specializations via neuroligins. *Cell* *119*, 1013–1026.
- Graf, E.R., Kang, Y., Hauner, A.M., and Craig, A.M. (2006). Structure function and splice site analysis of the synaptogenic activity of the neurexin-1 beta LNS domain. *J. Neurosci.* *26*, 4256–4265.
- Gutiérrez, R.C., Flynn, R., Hung, J., Kertesz, A.C., Sullivan, A., Zamponi, G.W., El-Husseini, A., and Colicos, M.A. (2009). Activity-driven mobilization of postsynaptic proteins. *Eur. J. Neurosci.* *30*, 2042–2052.
- Heine, M., Thoumine, O., Mondin, M., Tessier, B., Giannone, G., and Choquet, D. (2008). Activity-independent and subunit-specific recruitment of functional AMPA receptors at neurexin/neuroigin contacts. *Proc. Natl. Acad. Sci. USA* *105*, 20947–20952.
- Iida, J., Hirabayashi, S., Sato, Y., and Hata, Y. (2004). Synaptic scaffolding molecule is involved in the synaptic clustering of neuroligin. *Mol. Cell. Neurosci.* *27*, 497–508.
- Irie, M., Hata, Y., Takeuchi, M., Ichtchenko, K., Toyoda, A., Hirao, K., Takai, Y., Rosahl, T.W., and Südhof, T.C. (1997). Binding of neuroligins to PSD-95. *Science* *277*, 1511–1515.
- Ko, J., Zhang, C., Arac, D., Boucard, A.A., Brunger, A.T., and Südhof, T.C. (2009). Neuroligin-1 performs neurexin-dependent and neurexin-independent functions in synapse validation. *EMBO J.* *28*, 3244–3255.
- Legate, K.R., and Fässler, R. (2009). Mechanisms that regulate adaptor binding to beta-integrin cytoplasmic tails. *J. Cell Sci.* *122*, 187–198.
- Leone, P., Comoletti, D., Ferracci, G., Conrod, S., Garcia, S.U., Taylor, P., Bourne, Y., and Marchot, P. (2010). Structural insights into the exquisite selectivity of neurexin/neuroigin synaptic interactions. *EMBO J.* *29*, 2461–2471.
- Levinson, J.N., Chéry, N., Huang, K., Wong, T.P., Gerrow, K., Kang, R., Prange, O., Wang, Y.T., and El-Husseini, A. (2005). Neuroligins mediate excitatory and inhibitory synapse formation: involvement of PSD-95 and neurexin-1beta in neuroligin-induced synaptic specificity. *J. Biol. Chem.* *280*, 17312–17319.
- Levinson, J.N., Li, R., Kang, R., Moukhles, H., El-Husseini, A., and Bamji, S.X. (2010). Postsynaptic scaffolding molecules modulate the localization of neuroligins. *Neuroscience* *165*, 782–793.
- Lim, S.-H., Kwon, S.-K., Lee, M.K., Moon, J., Jeong, D.G., Park, E., Kim, S.J., Park, B.C., Lee, S.C., Ryu, S.-E., et al. (2009). Synapse formation regulated by protein tyrosine phosphatase receptor T through interaction with cell adhesion molecules and Fyn. *EMBO J.* *28*, 3564–3578.
- Meier, J., Vannier, C., Sergé, A., Triller, A., and Choquet, D. (2001). Fast and reversible trapping of surface glycine receptors by gephyrin. *Nat. Neurosci.* *4*, 253–260.
- Miyamoto, S., Akiyama, S.K., and Yamada, K.M. (1995). Synergistic roles for receptor occupancy and aggregation in integrin transmembrane function. *Science* *267*, 883–885.
- Mondin, M., Labrousse, V., Hosy, E., Heine, M., Tessier, B., Levet, F., Poujol, C., Blanchet, C., Choquet, D., and Thoumine, O. (2011). Neurexin-neuroigin adhesions capture surface-diffusing AMPA receptors through PSD-95 scaffolds. *J. Neurosci.* *31*, 13500–13515.
- Mukherjee, K., Sharma, M., Urlaub, H., Bourenkov, G.P., Jahn, R., Südhof, T.C., and Wahl, M.C. (2008). CASK Functions as a Mg²⁺-independent neurexin kinase. *Cell* *133*, 328–339.
- Nam, C.I., and Chen, L. (2005). Postsynaptic assembly induced by neurexin-neuroigin interaction and neurotransmitter. *Proc. Natl. Acad. Sci. USA* *102*, 6137–6142.
- Okabe, S., Kim, H.D., Miwa, A., Kuriu, T., and Okado, H. (1999). Continual remodeling of postsynaptic density and its regulation by synaptic activity. *Nat. Neurosci.* *2*, 804–811.
- Okabe, S., Urushido, T., Konno, D., Okado, H., and Sobue, K. (2001). Rapid redistribution of the postsynaptic density protein PSD-95 (Homer 1c) and its differential regulation by NMDA receptors and calcium channels. *J. Neurosci.* *21*, 9561–9571.
- Opazo, P., Labrecque, S., Tigaret, C.M., Frouin, A., Wiseman, P.W., De Koninck, P., and Choquet, D. (2010). CaMKII triggers the diffusional trapping of surface AMPARs through phosphorylation of stargazin. *Neuron* *67*, 239–252.
- Palmer, A., Zimmer, M., Erdmann, K.S., Eulenburg, V., Porthin, A., Heumann, R., Deutsch, U., and Klein, R. (2002). EphrinB phosphorylation and reverse signaling: regulation by Src kinases and PTP-BL phosphatase. *Mol. Cell* *9*, 725–737.
- Peixoto, R.T., Kunz, P.A., Kwon, H., Mabb, A.M., Sabatini, B.L., Philpot, B.D., and Ehlers, M.D. (2012). Transsynaptic signaling by activity-dependent cleavage of neuroligin-1. *Neuron* *76*, 396–409.
- Pouloupoulos, A., Aramuni, G., Meyer, G., Soykan, T., Hoon, M., Papadopoulos, T., Zhang, M., Paarmann, I., Fuchs, C., Harvey, K., et al. (2009). Neuroligin 2 drives postsynaptic assembly at perisomatic inhibitory synapses through gephyrin and collybistin. *Neuron* *63*, 628–642.
- Pouloupoulos, A., Soykan, T., Tuffy, L.P., Hammer, M., Varoqueaux, F., and Brose, N. (2012). Homodimerization and isoform-specific heterodimerization of neuroligins. *Biochem. J.* *446*, 321–330.
- Rikova, K., Guo, A., Zeng, Q., Possemato, A., Yu, J., Haack, H., Nardone, J., Lee, K., Reeves, C., Li, Y., et al. (2007). Global survey of phosphotyrosine signaling identifies oncogenic kinases in lung cancer. *Cell* *131*, 1190–1203.
- Saint-Michel, E., Giannone, G., Choquet, D., and Thoumine, O. (2009). Neurexin/neuroigin interaction kinetics characterized by counting single cell-surface attached quantum dots. *Biophys. J.* *97*, 480–489.
- Saiyed, T., Paarmann, I., Schmitt, B., Haeger, S., Sola, M., Schmalzing, G., Weissenhorn, W., and Betz, H. (2007). Molecular basis of gephyrin clustering at inhibitory synapses: role of G- and E-domain interactions. *J. Biol. Chem.* *282*, 5625–5632.
- Scheiffele, P., Fan, J., Choih, J., Fetter, R., and Serafini, T. (2000). Neuroligin expressed in nonneuronal cells triggers presynaptic development in contacting axons. *Cell* *101*, 657–669.
- Schlüter, O.M., Xu, W., and Malenka, R.C. (2006). Alternative N-terminal domains of PSD-95 and SAP97 govern activity-dependent regulation of synaptic AMPA receptor function. *Neuron* *51*, 99–111.
- Schnell, E., Sizemore, M., Karimzadegan, S., Chen, L., Brecht, D.S., and Nicoll, R.A. (2002). Direct interactions between PSD-95 and stargazin control synaptic AMPA receptor number. *Proc. Natl. Acad. Sci. USA* *99*, 13902–13907.
- Shipman, S.L., Schnell, E., Hirai, T., Chen, B.-S., Roche, K.W., and Nicoll, R.A. (2011). Functional dependence of neuroligin on a new non-PDZ intracellular domain. *Nat. Neurosci.* *14*, 718–726.

- Sturgill, J.F., Steiner, P., Czervionke, B.L., and Sabatini, B.L. (2009). Distinct domains within PSD-95 mediate synaptic incorporation, stabilization, and activity-dependent trafficking. *J. Neurosci.* 29, 12845–12854.
- Südhof, T.C. (2008). Neuroligins and neurexins link synaptic function to cognitive disease. *Nature* 455, 903–911.
- Sumioka, A., Yan, D., and Tomita, S. (2010). TARP phosphorylation regulates synaptic AMPA receptors through lipid bilayers. *Neuron* 66, 755–767.
- Takahashi, H., Arstikaitis, P., Prasad, T., Bartlett, T.E., Wang, Y.T., Murphy, T.H., and Craig, A.M. (2011). Postsynaptic TrkC and presynaptic PTP σ function as a bidirectional excitatory synaptic organizing complex. *Neuron* 69, 287–303.
- Varley, Z.K., Pizzarelli, R., Antonelli, R., Stancheva, S.H., Kneussel, M., Cherubini, E., and Zacchi, P. (2011). Gephyrin regulates GABAergic and glutamatergic synaptic transmission in hippocampal cell cultures. *J. Biol. Chem.* 286, 20942–20951.
- Varoqueaux, F., Jamain, S., and Brose, N. (2004). Neuroligin 2 is exclusively localized to inhibitory synapses. *Eur. J. Cell Biol.* 83, 449–456.
- Washbourne, P., Bennett, J.E., and McAllister, A.K. (2002). Rapid recruitment of NMDA receptor transport packets to nascent synapses. *Nat. Neurosci.* 5, 751–759.